A quantitative examination of lightning as a predictor of peak winds in tropical cyclones

Ian C. Whittaker[1], Emma Douma[1], Craig J. Rodger[1], and Timothy J. C. H. Marshall[1]

[1] Department of Physics, University of Otago, Dunedin, New Zealand

Abstract We use the World Wide Lightning Location Network to investigate lightning strike variations in 8 years of categories 4 and 5 tropical cyclones. A cross-correlation analysis is performed between the lightning and maximum sustained wind variations, giving lag and lead times related to the peak linear correlation for each tropical cyclone. A previous study of 58 cyclones by Price et al. (2009) is reexamined using the International Best Track Archive for Climate Stewardship database for the maximum sustained wind speeds of each tropical cyclone showing a moderate to strong correlation between lightning and wind variations. An 8 year data set of 144 tropical cyclones are analyzed in the same way, with a 10° square window, giving similar results to the smaller data set. Using a radial lightning collection window of < 500 km, we confirm the general results of previous studies that lightning can be used on a ~1 day timescale to predict the evolution of the winds in tropical cyclones. Investigation of different lightning collection window sizes indicates that the lightning lead times are highly dependent upon the window size. Smaller collection windows have modal lightning lead times of ~2.75 and 0 days, indicating that the lightning location inside the cyclone is as important as the total lightning variation. We have also performed a fixed time lag correlation which shows that preexisting knowledge of what time lag to use is needed in order to use this approach as a predictive tool.

1. Introduction

1.1. Overview

Accurate forecasting of tropical cyclones is of great importance, especially for communities where landfall might occur due to the extreme damage caused. The most likely future path of a tropical cyclone can be modeled [e.g., *McAdie and Lawrence*, 2000] with low track error (300 km for the North Atlantic in 2000–2005 for a 48 h forecast [*DeMaria et al.*, 2007], ~150 km for 48 h forecasts in 2014 [*National Hurricane Center*, 2014]). Improvements to these forecasts has meant that the National Hurricane Center track and intensity forecasts increased from 3 days to 5 days in 2003, and warnings being issued on a 36 h time frame in 2010. Tropical cyclones deviating from the forecast are monitored and tested to improve the limitations of such forecasting [e.g., *Brennan and Majumdar*, 2011]. However, while the global forecasting models are successful at predicting the track of the cyclone, they are not as good at predicting the wind intensities [*Rappaport et al.*, 2009; *DeMaria et al.*, 2007].

Globally, one of the most severe tropical cyclones on record to date occurred in 2013 in the Philippines. Typhoon Yolanda (Haiyan) had wind speeds in excess of 300 km h^{-1} [*Schiermeier*, 2013] and caused over 6300 deaths (with a further 29,000 people injured or missing) with damages totaling U.S. $2 billion [*National Disaster Risk Reduction and Management Council*, 2014]. *Romps et al.* [2014] have recently linked lightning flash rates to increasing temperature in global climate models, suggesting a 12% increase in flash rates per degree Celsius of warming over the U.S. This increasing lightning activity is an unknown factor, in terms of addition to a noise background or strike rate enhancement, and has the potential to be beneficial if the flash rate can be used as a predicting tool in tropical cyclones.

The first attempts to track tropical cyclones using atmospheric electrical activity were made in 1938; it was concluded from a study of six Atlantic storms that "static" (electrical activity) did not appear in the center of the storm but rather on its edges [*Sashoff and Roberts*, 1942]. Lightning has also been detected during aircraft penetration of storm interiors, although this came under debate as being caused by the aircraft themselves [*Black and Hallett*, 1986]. The first study to investigate the links between lightning and wind speed intensity [*Lyons and Keen*, 1994] determined that "supercell" convective clouds may lead to an increase in storm intensity and in turn, cloud to ground lightning discharges. This study found that lightning occurring in the
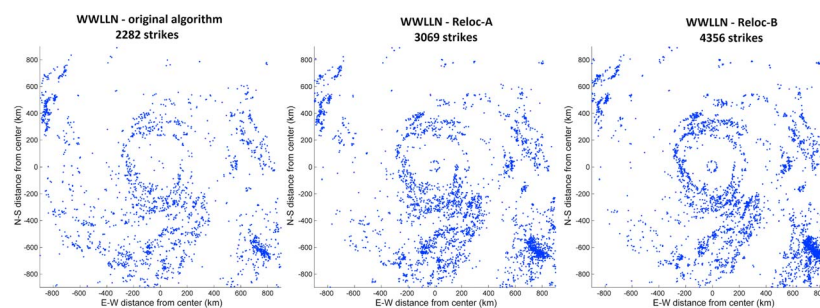
Figure 1. An example of the changes that the different WWLLN algorithms have on lightning detection in tropical cyclones. (left to right) Each panel shows a 24 h storm-centered plot of Hurricane Katrina on 28 August 2005.

eyewalls of two case study storms preceded periods of storm intensification where usually there would be very little lightning activity. Lightning in the eyewall was later characterized as rare, requiring updrafts stronger than 10 m s^{-1}, and linked to mixed-phase regions containing ice and supercooled water [*Black and Hallett*, 1999]. *Willis et al.* [1994] showed that a rapid electric field gradient is formed when the tropical cyclone exhibits strong vertical velocities with charge separation forming from the interaction of graupel and small ice particles. Recently, researchers have been investigating the lightning within tropical cyclones in an attempt to improve our understanding of storm structure and the changes in wind intensity [e.g., *Thomas et al.*, 2010; *Reinhart et al.*, 2014]. *Fierro and Reisner* [2011] also linked lightning activity to the latent heat release within tropical cyclones.

Price et al. [2009] performed an analysis of 58 categories 4 and 5 tropical cyclones and concluded that lightning flash rates have a typical 30 h lead on the maximum winds in a tropical cyclone. In a similar style, *Pan et al.* [2014] performed a study of super and weak typhoons which resulted in lightning lead times of 30 and 60 h, respectively. *Abarca and Corbosiero* [2011] showed that lightning flash density is higher when tropical cyclone wind speeds are increasing, leading to a study of rapid intensification changes by *DeMaria et al.* [2012], who concluded that lightning can be used to improve short term (24 h) predictions of wind intensification.

Our paper reexamines the study of *Price et al.* [2009], and we aim to test the validity of their conclusions and extend their method to a much larger storm data set. As well as expanding the number of storms we also perform a fixed time lag analysis for a range of times. We also include a table of probabilities that the peak winds occur within a set number of hours from the peak in lightning strike rate. In this study we will henceforth refer to all high-category tropical storms as tropical cyclones, regardless of their basin of origin and thus include hurricanes and typhoons.

1.2. Data Sources

We are using data from the International Best Track Archive for Climate Stewardship (IBTrACS v03r05), a World Meteorological Organization Tropical Cyclone Programme endorsed database for the wind, pressure, and location of the tropical cyclones [*Knapp et al.*, 2010]. We restrict our observations to those recorded by World Meteorological Organization endorsed stations. We use lightning data (version Reloc-B) from the ground based World Wide Lightning Location Network (WWLLN). WWLLN is a global network consisting of over 65 detection stations using very low frequency (3–30 kHz) receivers to detect lightning flashes using a time-of-group-arrival technique. A recent description of the WWLLN network operation and characteristics can be found in *Hutchins et al.* [2012] and at http://wwlln.net.

1.3. WWLLN Algorithm Version Differences

An important factor in using WWLLN data is the lightning detection algorithm version that was used to process the timing observations to produce lightning locations. As previously stated we are using Reloc-B which is the third algorithm version to be used by WWLLN. As an example of the differences between the algorithm versions we have created an 1800 × 1800 km 24 h storm-centered lightning distribution plot for Hurricane Katrina on 28 August 2005, in a similar style to *Solorzano et al.* [2008]. Katrina plots for each of the WWLLN algorithms are shown in Figure 1, with the original algorithm shown in the left panel, Reloc-A in the middle panel, and Reloc-B in the right panel. The number of strikes included increases from 2282 to 3069 and up to 4356 for the original, Reloc-A and Reloc-B algorithms, respectively. This shows that Reloc-B produced almost double the number of lightning strikes as the original algorithm did for the same storm and

time period. It should be noted by looking at Figures 1 (left) and 1 (right) that it also removed a small number of strikes in the (−600, −200) region. A higher flash rate detection efficiency could lead to higher flash magnitudes which should produce better defined changes in activity. While the frequency of flash rates increase we do not expect this to change the shape of the flash distribution over time and investigation of Hurricane Dennis (see section 2.2) shows only small changes in the shape of the lightning flash distribution between Reloc-A and Reloc-B. This result is consistent with *Jacobson et al.* [2006] who used WWLLN data from 2005 to show that the improving detection efficiency alters the total lightning but is unlikely to significantly affect the lightning variation.

2. Recreating the Results of *Price et al.* [2009]

2.1. Overview of Results and Conclusions

Price et al. [2009] (hereafter referred to as Price) investigated a data set of 58 tropical cyclones for 2005 to 2007 which were classified as categories 4 and 5 (>114 kt) on the Saffir-Simpson scale [*Saffir*, 1973; *Simpson*, 1974]. Their tropical cyclone subset had 40% of cyclones in the West Pacific and included cyclones in the West Atlantic, East Pacific, and Indian Oceans. Price used WWLLN to determine the total lightning within the tropical cyclone using a 10° × 10° square window centered on the eye. The maximum sustained wind and pressure data for each cyclone was taken from the National Hurricane Center and the Joint Typhoon Warning Center with 6 h resolution and then smoothed using a 24 h running average. The same averaging method was used on the lightning data by collating the submicrosecond resolution lightning strike data into 6 h totals and then applying a 24 h running average. A comparison between average wind speeds and lightning strike rate was then performed.

Price reported a positive correlation ($r = 0.82$) of strong significance (>90%) between the variation in winds and lightning for 56 of the 58 cyclones. The peak correlation had a variable time offset, with the lightning leading the winds by as much as 6 days in some cases, and in others the lightning lagged the winds by up to 3 days. The mean and median lead time of the lightning variability was reported as 30 h. When each tropical cyclone was compared using this 30 h lead time, 31 events showed a positive correlation with 19 of these showing a statistical significance > 90%. We begin by comparing the IBTrACS database to the WWLLN lightning data for the Price storm set.

2.2. Reanalysis of the Data

Using IBTrACS, 38 of the 58 cyclones used by Price have a maximum sustained wind speed below the 114 kt category 4 limit defined by the Saffir-Simpson scale. Using tropical cyclone "Sonca" as an example, Price's supplementary material showed that the smoothed peak winds reach ~115 kt, whereas the unsmoothed IBTrACS maximum wind speed for this cyclone is only 100 kt (the smoothed peak is 90 kt). The Sonca winds in Price develop the same way over time as the IBTrACS data, showing a single wind peak just before 25 April 2005, although there is a constant offset in wind speeds at all times. It should be noted that these 38 cyclones with a maximum sustained wind <114 kt still fall under the Hong Kong Observatory classification of a "severe typhoon" (equivalent to a category 4 classification with a lower limit of 81 kt). However, we note that the magnitude differences between Price and IBTrACS are not important in this study as the cross-correlation procedure to determine peak lag and lead times involves subtracting the mean from each data set, centering the data around 0 regardless of its original magnitude.

We begin, in a similar style to Price, with Hurricane Dennis. This tropical cyclone was tracked between 5 and 15 July 2005. To perform the running average, we initially attempted using the average of four time bins (a 24 h period); however, an even number of bins requires an interpolated time value to be used. This interpolation was tested and did not reproduce the Price wind and pressure results. The number of bins was increased to 5 (a 30 h period), allowing use of whole time bins and correctly reproducing the wind and pressure variation. The wind and pressure variations in Hurricane Dennis is shown in panel Figure 2a. However, the lightning strike variation using the same 30 h average approach produces different results from Price as shown in Figure 2b. The results from Price are reproduced in Figures 2c and 2d for comparison to Figures 2a and 2b, respectively. The wind and pressure plot we have produced in Figure 2a looks very similar to the Price wind and pressure in Figure 2c; this suggests that the IBTrACS database for wind and pressure is equivalent to the database that Price used and that we have reproduced Price's method correctly. We see a similar shape in the smoothed lightning activity with the second peak at approximately the same activity rate as Price. However, the initial lightning activity peak is lower than Figure 2d, and the third peak is much higher. We have attempted
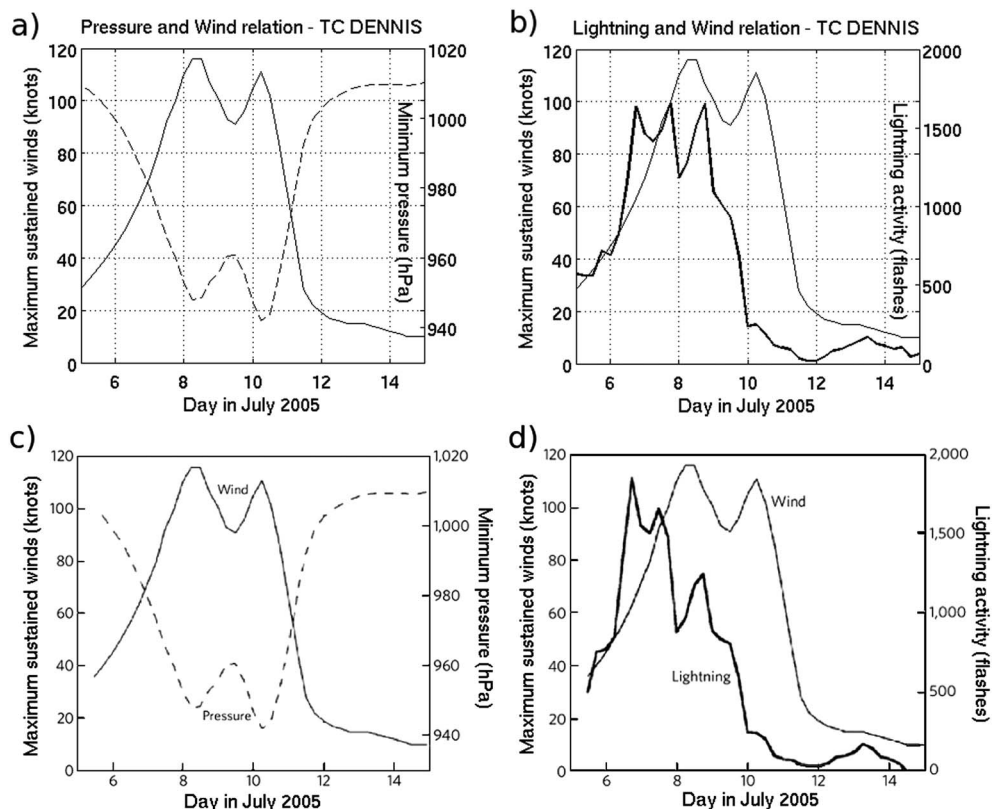
Figure 2. The wind, pressure, and lightning during Hurricane Dennis in 2005. (a and b) Our reproduction of the analysis of Hurricane Dennis using IBTrACS and a 30 h lightning binning procedure. (c and d) Reproduced from Figure 2 in Price and show the same data processed by these authors. Reprinted by permission from Macmillan Publishers Ltd: [NATURE] (Price, Asfur, and Yair), copyright (2009). Shown in Figures 2a and 2c are the 30 h smoothed wind (solid) and pressure (dashed) in Hurricane Dennis. Shown in Figures 2b and 2d are the 30 h smoothed wind (thin line) and lightning (thick line).

multiple methods to reproduce Price's values including the following: median averaging, larger and smaller time windows to average over, different total lightning flash bin sizes, introducing bias to the averaging, and using older WWLLN products with no improvement. The reproduction of Hurricane Dennis has been independently performed by three of the authors, and all have reproduced the variability shown in Figure 2b. We perform a cross correlation of the wind and lightning strike data seen in our Figure 2, taking the time difference associated with the peak value, then shift the two data sets and perform a linear correlation. We use a t test with a null hypothesis (Student's t test) to calculate the significance value. For Hurricane Dennis, we find that the lightning leads the winds by 30 h with a correlation of 0.96 and a statistical significance over 99.9%. This is very close to the Price values for this storm of 24 h and a correlation of 0.95. The small differences are most likely to arise from our inability to perfectly reproduce the Price lightning curve. The direct wind to pressure correlation was also calculated giving a linear correlation value of −0.98.

We repeated this process for all 58 tropical cyclones in the Price data set but included two extra conditions. The first condition is that the first and last two time bins of the wind and lightning data are removed after the running average is performed. This removal ensures that the data points which do not have sufficient neighboring values to average over are not included. The second condition is that the cross-correlation time difference between the lightning and wind values are limited to +6 days and −3 days as Price reports no differences outside these limits. Our analysis of the direct wind and pressure relation is highly negatively correlated as we expect from nonindependent variables, with a mean correlation of −0.988 and median correlation of −0.993. The varying lightning to wind correlations for the Price cyclones are given in Figure 3a. Each tropical cyclone is given a symbol similar to Price's Figure 4, based on the statistical significance of the result as shown in the legend. The average correlation of the 58 cyclones has a mean of 0.72 and median of 0.74, in comparison to the mean correlation value of 0.82 given by Price. Three cyclones ("Khanun," "Sidr," and "Wipha")
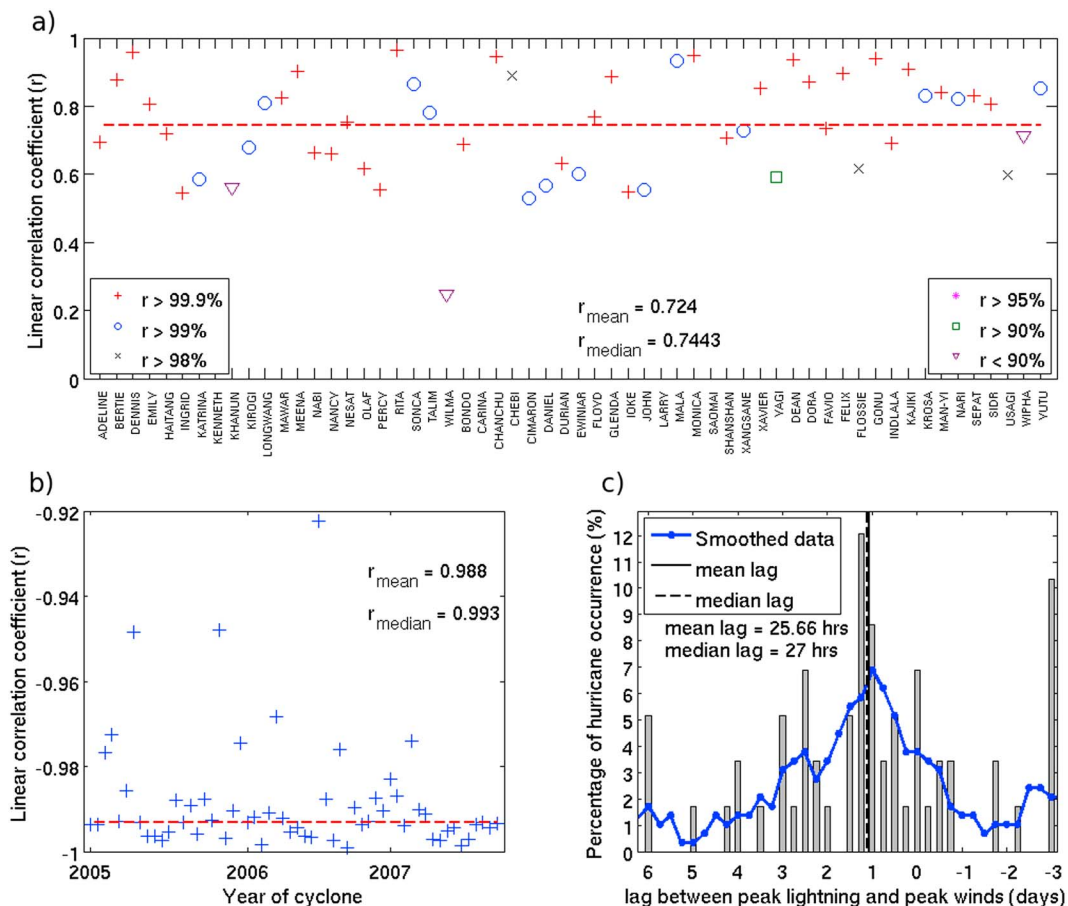
Figure 3. Reproduction of the *Price et al.* [2009] study using IBTrACS and WWLLN, with a 10° square window. (a) The linear correlation coefficients of the wind to lightning variation for each of Price's 58 tropical cyclones. The symbol indicates the statistical significance. (b) The wind to pressure linear correlation for each of the 58 cyclones. (c) The distribution of peak correlation time lags (a 30 h smoothing is shown by the blue solid line).

have a statistical significance < 90% (~85% for all three). Our analysis of the direct wind and pressure relation is shown in Figure 3b and is highly negatively correlated as expected. The mean linear correlation of the wind to pressure variation is −0.988, and the median correlation is −0.993.

Figure 3c shows the distribution of the tropical cyclone lag data for comparison to Price's Figure 3. Here a positive lag indicates that the lightning variation leads the wind variation. The time resolution of the lag distribution is set to 6 h (grey bars). Again, the distribution does not match the specific values seen in Price. A summation of the distribution in Figure 3 in Price exceeds 200%, suggesting some errors in this figure. Despite the difference, we still find mean and median lag times close to the 30 h values reported by Price. The mean lag time for our analysis is +24 h with a median value of +27 h. These average lag times are indicated in Figure 3c by the solid (mean) and dashed (median) lines. As a final test the three cyclones with statistical significance less than 90% are removed and the averages recalculated, giving little change to the mean lag (+24 h) and providing a median lag of +24 h. Smoothing the lag distribution data across five bins (30 h, solid blue line) produces a distribution which looks closer to Price's Figure 3.

We conclude that while the results presented by Price cannot be completely reproduced, the reanalysis does indicate that there is a moderate to strong correlation between lightning and wind variations, with the lightning leading the wind by 30 h.

3. Repeating the Method for a Larger Subset of Storms
3.1. Identifying Tropical Cyclones
The analysis approach from section 2.2 is now extended to a larger and longer tropical cyclone data set initially to test if the 3 year subset is a representative sample. We then use this larger data set to investigate

Table 1. The Intensity Classification for Categories of Tropical Cyclones in Different Regions Based Upon Maximum Sustained Wind Speeds[a]

Category	Hurricanes	Typhoon	Australian TC	Indian TC
1	> 64	> 34	> 34	> 34 (3)
2	> 83	> 48	> 48	> 48 (4)
3	> 96	> 64	> 64	> 64 (5i)
4	> 113	> 81	> 86	> 91 (5ii)
5	> 137	> 100	> 107	> 120 (6)

[a]The categories defined by the New Delhi Regional Specialized Meteorological Centre are more numerous, and the equivalent categories are included in brackets. Descriptions of the basin locations are given in the text. Wind speeds are converted to knots.

different lightning collection windows. Classification of cyclones by wind intensity depends upon its basin of origin. NOAA's Hurricane Research Division identifies seven basins of origin for tropical cyclones which can be split into five regions. These regions are hurricanes (West Atlantic and East Pacific north of the equator to the International Dateline), typhoons (International Dateline to 110° longitude north of the equator), Australian tropical cyclone (TC) (100° eastward to −120° longitude, south of the equator), Indian TC (30° to 100° longitude both sides of the equator), and any other location (including the Mediterranean, which has been known to rarely generate events which appear to be tropical cyclones [*Emanuel*, 2005]). The intensity classifications for each area are included in Table 1 with the maximum sustained wind speeds converted to knots. The difference in maximum sustained wind speed thresholds needs to be considered as average maximum sustained wind speeds vary strongly between basins (as shown in Figure 4). If we applied the hurricane wind thresholds, very few categories 4 and 5 cyclones that occurred in other basins would have been included. The intention of our study is to expand the tropical cyclones of Price in both time and basin origin. The hurricane classification is from the latest update of the Saffir-Simpson wind scale at the National Hurricane Center, the typhoon classification is taken from the Hong Kong Observatory and the Australian classification is taken from the Australian Bureau of Meteorology. The classifications for the Indian Ocean basins are taken from the Indian Regional Specialized Meteorological Center, who uses seven categories (1 to 4, 5(i), 5(ii), and 6) for tropical storms. These have been matched up to be consistent with those of other agencies in Table 1. For our larger cyclone data set only categories 4 and 5 tropical cyclones (equivalent to 5(ii) and 6 in the case of those with Indian Ocean basin of origin) will be included.

The basin of origin is determined by the latitude and longitude of the first maximum sustained wind speed data point in the IBTrACS database for each cyclone. We find 144 tropical cyclones which can be classified as category 4 or 5 between January 2005 and February 2013 (~20% of the tropical cyclone list for these dates). The initial position of the 144 tropical cyclones is shown in Figure 4 with each basin region boundary identified. The color of each start position represents the peak maximum sustained wind speed of the cyclone ranging from 85 to 160 kt. All 58 cyclones in the Price data set passed the minimum sustained wind speeds to be classed as a category 4 or 5 tropical cyclone using the classifications in Table 1 and are included in this 8 year data set, along with an extra five cyclones from this time period which were also identified and included.
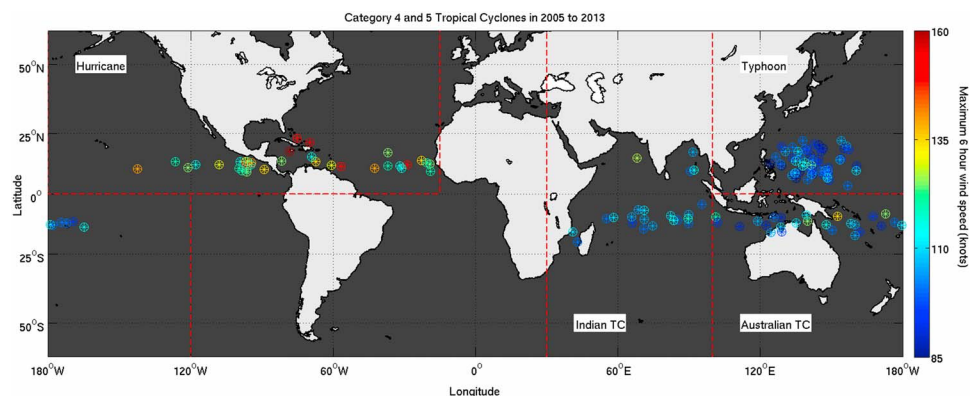

Figure 4. A global map showing the starting point of each of the 144 tropical cyclones identified in the 2005 to 2013 database as category 4 or 5. The color of the marker indicates the cyclone maximum sustained wind speed.
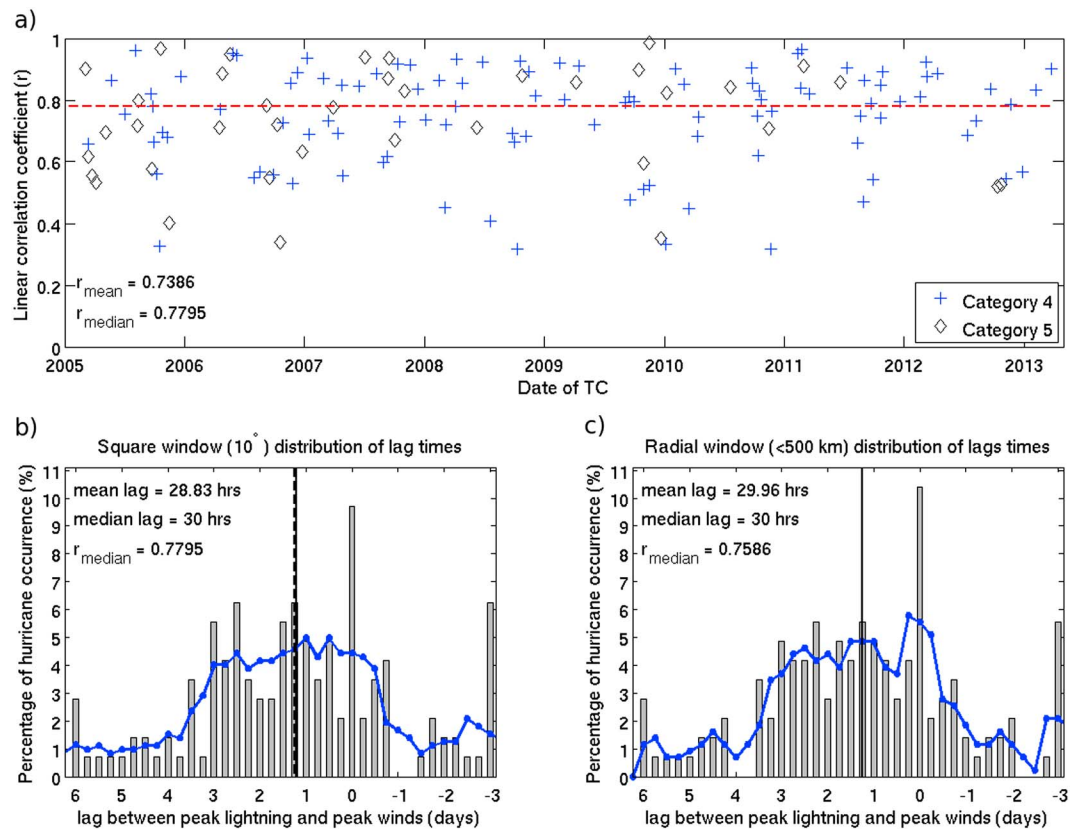
Figure 5. Data from the extended 8 year data set covering January 2005 to February 2013. (a) The optimal linear correlation of the wind to lightning variation for each of the 144 cyclones. Symbols correspond to the category of the cyclone. (b) The distribution of peak correlation time lags using the 10° square window centered on the cyclone to collect lightning strikes. (c) The distribution of peak correlation time lags using a < 500 km radial window centered on the cyclone.

3.2. Analysis of the 8 Year Tropical Cyclone Data Set

Figure 5a shows the 8 year data set in a similar style to Figure 3a. The *x* axis indicates the start date of the tropical cyclone instead of the name of the storm. Each data point symbol relates to the category of the tropical cyclone as this provides more relevant information than the significance symbols. The linear correlation and optimal lag was compared for the maximum sustained wind speed, basin of origin, and the mean/median/total lightning strikes in the cyclone with no significant differences observable. There are two tropical cyclones not plotted which have a negative correlation value ("Carina" in 2006, $r = -0.15$ and "Roke" in 2011, $r = -0.35$). The mean (0.74) and median (0.78) linear correlations are very close to the 3 year data set of Price shown in Figure 3a, indicating that the Price tropical cyclones are a fair sample of the larger population. Figure 5b shows the distribution of lag times in a similar style to Figure 3c. Once again the mean (29 h) and median (30 h) lags are very similar to the ~1 day timescale discussed in both Price and *DeMaria et al.* [2012]. The supporting information included with this manuscript includes the name, basin, linear correlation, and lags for each of the 144 cyclones used in this study.

3.3. Lightning Strike Collection Window

To collect the 6 h lightning strike totals, Price used a 10° × 10° square window. Up to now we also used the same window size and shape but now investigate a window more suited to the shape of a tropical cyclone. The 10° × 10° square is changed to a circular window with a radius set in kilometers rather than degrees. At the equator 10° is ~1100 km so we rerun the analysis on the 8 year data set for radii ranging from 500 km down to 100 km in 100 km increments as well as a 50 km radius. A range of toroidal rings were also calculated.

A comparison of the circular to square window is performed by investigating the 500 km radius circular window centered on the cyclone. The distribution of lags for this radial window is shown in Figure 5c.
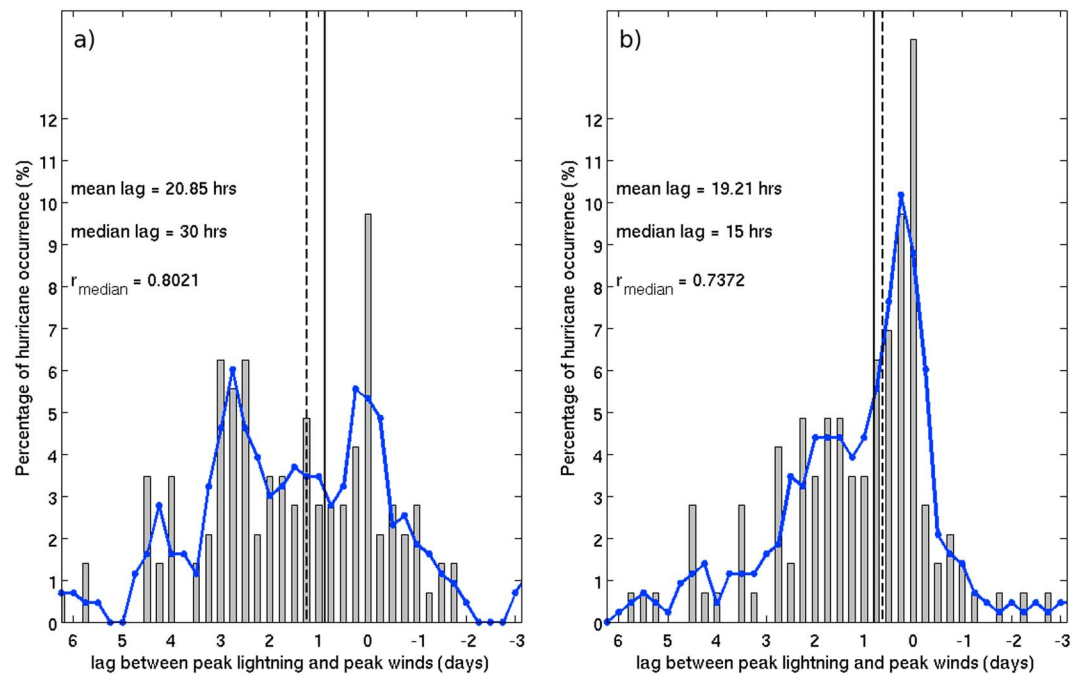
Figure 6. The 8 year data set analyzed using a circular window, in km rather than degrees, centered on the storm. (a) The distribution of lags using a < 300 km radial distance window for the lightning detection. (b) The distribution of lags using a < 50 km radial distance; this distance is most likely composed of eyewall lightning.

As expected there are only small changes in the results between the 500 km radial and 10° square window, with the shape of the distributions showing strong similarities. The circular window giving both mean and median lags of 30 h (in comparison to 29 and 30 h from the square window) and the median linear correlation was 0.76.

Table 2. A Summary of the Results From Each Lightning Collection Window[a]

Window Size	Median Lag	Mean Lag	Median Correlation	Mean Correlation
		Square Window		
10°	30	28.8	0.78	0.74
	Circular Window (Cross-Correlation Limits of +6 and −3 days)			
< 500 km	30	29.9	0.76	0.66
		Circular Window (Unlimited)		
< 500 km	15	2.63	0.78	0.71
< 400 km	18	5.58	0.79	0.71
< 300 km	27	14.4	0.80	0.76
< 200 km	27	16.1	0.75	0.68
< 100 km	21	15.3	0.74	0.69
< 50 km	18	18.6	0.74	0.70
200 to 300 km	18	10.9	0.78	0.72
150 to 300 km	24	15.2	0.80	0.76
100 to 300 km	27	14.6	0.79	0.74
50 to 300 km	30	16.6	0.78	0.76
100 to 200 km	30	14.5	0.74	0.68
50 to 200 km	36	18.7	0.74	0.70
50 to 100 km	27	14.5	0.74	0.69

[a]Lags are measured in hours where a positive lag implies the lightning variation leads the wind variation. The correlations are the average of the peak linear correlations for all 144 tropical cyclones.

Table 3. The Mean and Median Correlations of the 8 Year Data Set Split by Basin and Wind Speed Using Fixed Time Lags[a]

	Fixed Lag Time				# TC	
	0 h	6 h	30 h	66 h	0 h, 6 h, and 30 h	66 h
All TC median	−0.04	0.02	0.11	0.23	144	139
All TC mean	0.00	0.03	0.10	0.19		
Hurricane median	0.11	0.19	0.33	0.38	34	34
Hurricane mean	0.16	0.20	0.30	0.29		
Typhoon median	−0.09	0.01	0.14	0.23	57	54
Typhoon mean	−0.03	−0.00	0.03	0.09		
Australasian TC median	−0.17	−0.04	0.00	0.37	31	30
Australasian TC mean	−0.06	−0.03	0.13	0.24		
Indian TC median	−0.30	−0.28	−0.12	0.16	22	21
Indian TC mean	−0.08	−0.06	−0.04	0.18		
Wind ≥ 105 kt median	0.05	0.11	0.24	0.23	80	79
Wind ≥ 105 kt mean	0.05	0.09	0.19	0.21		
Wind < 105 kt median	−0.13	−0.07	0.02	0.26	64	60
Wind < 105 kt mean	−0.07	−0.04	0.00	0.15		

[a]The 66 h fixed lag has fewer tropical cyclones as some events do not have enough data to support a correlation at this time difference.

In section 2.2 we described an initial condition limiting the cross correlation to +6 and −3 days to match the Price approach. We now remove this limitation for analysis of the individual circular lightning collection windows. The lag distribution smoothing (e.g., Figures 5b and 5c) is also reduced to a more conservative three-bin distance (18 h). The cross correlation and linear correlation were performed for each cyclone and lightning radial distance window described above. The 300 km radius window resulted in the highest linear correlation of lightning to wind variability with $r = 0.80$, shown in Figure 6a. Each radial distance collection window with the average correlations and lags are shown in Table 2. Investigation of the < 500 km radial window shows that the conditions implemented to reproduce Price (limiting the peak lag to between +6 and −3 days) makes a large difference to the average lag time. The lags found outside the limit times could be caused by a failure of the cross-correlation procedure, and we investigate this in section 4.

3.4. Fixed Time Lag Correlations

In the previous section we have shown that a circular window with a radius of 300 km produces the highest average correlation. In Figure 6a the distribution is bimodal with a mean and median value sitting between the modal peaks. As it is not possible to know which lag to use on a case by case basis, we proceed to calculate correlations for fixed time lags. These are related to the peaks in the distribution, and we test 0 h (modal value), 6 h (modal smoothed peak), 30 h (median value), and 66 h (second modal smoothed peak).

The average results of this fixed time lag correlation analysis are shown in Table 3. Each row gives the mean and median correlations for each fixed time. Averages by basin and wind speed are also included in the table. It should be noted that five tropical cyclones did not contain a long enough time series to be able to perform a 66 h lag successfully, and these cyclones have been removed for this particular fixed time correlation. The results in Table 3 show that the best median correlation for all cyclones comes from the 66 h fixed time lag. This is also true for individual basins. However, we found this did not hold when we investigated the maximum sustained wind speed of the cyclones. The median maximum sustained wind speed of all cyclones was 105 kt, and so the data set was split on either side of this median. The tropical cyclones with maximum sustained wind speeds ≥ 105 kt showed the highest median correlation for a 30 h lag, although the 66 h lag was only slightly less correlated.

These data are shown in more detail in Figure 7, with the four fixed lag times in each panel (0 h at top left, 6 h at top right, 30 h at bottom left, and 66 h at bottom right). The solid black line shows the median correlation for all cyclones, and the red and blue dashed lines represent the fast and slow maximum sustained wind medians
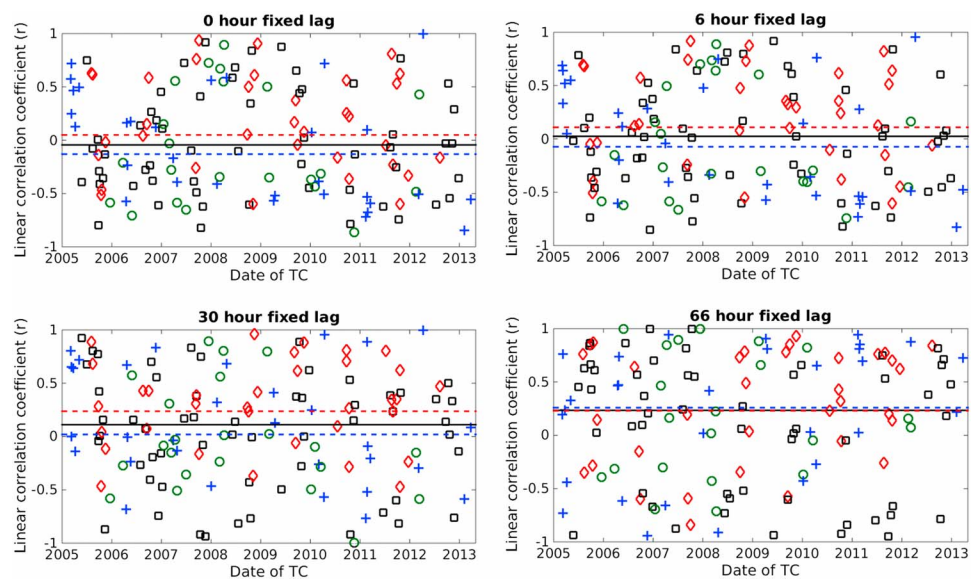
Figure 7. The 8 year data set analyzed with a 300 km circular window using fixed lag times of (top left) 0, (top right) 6, (bottom left) 30, and (bottom right) 66 h. Each tropical cyclone correlation is plotted with the basin location shown by symbols. Red diamonds are for hurricanes, black squares are for typhoons, blue crosses for Australasian basin origin tropical cyclones, and green circles for tropical cyclones of Indian Ocean basin origin. The red dashed lines show the median high wind speed (≥ 105 kt), while the blue dashed lines show the low wind speed medians. The black solid line shows the median correlation of all storms. Full values are given in Table 3.

given in Table 3. The spread of cyclone correlations is high for all four fixed lag times, although the medians clearly show that the highest correlations occur at the 66 h time period.

4. Discussion

We find broadly similar results to Price when we extend their approach to a longer 8 year data set of tropical cyclones. However, while the typical linear correlations give values in the range of 0.7 to 0.8, this does not necessarily indicate a true ability to match the evolving wind and lightning variation. Visual inspection of each of the 144 cyclones was performed to investigate the accuracy of the cross-correlation procedure. We plotted the following: the lightning against winds in a similar style to Figure 2b, the lag times against cross-correlation value, and the time shifted lightning data with wind data to determine the accuracy of the variation matching process. This inspection found three cyclones where the wind and lightning variation show no similarities and a further eight instances of the cross correlation performing poorly, giving a failure rate of ~8%, this relates to cyclones with low total lightning strikes and those with no changes over the cyclone lifetime. The two sources of cross-correlation failure were double-peaked winds with the lightning peak(s) linked to the wrong wind peak and lightning data which had a sharp lightning strike gradient at the beginning or end of the data (an example is shown in the supporting information). This large gradient in the 6 h lightning strike total, which occurs in cyclones with low total lightning strike rates, forced the cross-correlation procedure to match poorly and resulted in lags > 84 h and < −84 h (3.5 days). An example of a cross-correlation failure with this sharp lightning strike gradient is shown for tropical cyclone Daman in the supporting information.

In an attempt to improve the correlation method we switched to circular windows for lightning detection. The smoothing was also reduced down to three bins (18 h) as applying a 30 h lag

Table 4. The Percentage of Tropical Cyclones Showing a Wind Speed Peak Within a Set Time From the Lightning Strike Peak[a]

Time From Peak Lightning	# TC	% of All TC	% of Forward TC
≥ 0 h	99	69	100
≤ 6 h	9	6	9
≤ 12 h	14	10	14
≤ 24 h	24	17	24
≤ 48 h	45	31	45
≤ 66 h	61	43	61

[a]The first entry shows the number of events where the lightning peak follows the wind speed peak and hence can be potentially used for prediction purposes.

time along with the 30 h smoothing used in Price (and our subsequent reproduction) would introduce a large error. In section 3.3 we noted that a 300 km radius resulted in the best median linear correlation, shown in Figure 6a. While the mean and median lags show a value similar to that quoted by Price, the lags show a double peak distribution at +66 h (2.75 days) and 0 h, with these average values sitting between them. Taking the average provides little to no information in this specific case. We performed a fixed lag correlation analysis in section 3.4 looking at the full modal peak (0 h), both the smoothed modal peaks (6 and 66 h) and the median value of 30 h. The results shown in Table 3 and Figure 7 show that the highest correlations are for a fixed time lag of 66 h. The highest average correlations are 0.38 for hurricanes and 0.37 for Australasian basins with a 66 h lag.

We further investigate the bimodal peaks of Figure 6 by looking at radial distances smaller than 300 km. Figure 6b shows the < 50 km radial distance which has only a single clear peak between 0 and +6 h. *Molinari et al.* [1994] used a distance less than 40 km as corresponding to eyewall lightning in Hurricane Andrew, while *Zhang et al.* [2012] determined lightning at < 60 km was eyewall lightning. We can therefore assume that our < 50 km radial window is providing correlations predominately for eyewall lightning. *Molinari et al.* [1999] showed that lightning density in tropical cyclones is bimodal as a function of radial distance, with one distribution in the eyewall and the other in the rainband region (150–300 km). This double lightning distribution could be the main reason for the low average correlations in Table 3 as a double peak would lower correlations especially if the lightning enhancement is low. Investigation of other radial distances, including the 150–300 km region, provides no other single peaks in the lag distribution. When looking at the < 300 km circular window in Figure 6a, it is interesting to note that *Pan et al.* [2014] found a single modal lightning lag of +60 h (2.5 days) when looking at weak tropical cyclones in the Northwest Pacific (using a < 600 km radius window). *DeMaria et al.* [2012] also determined that inner core lightning outbreaks are "a signal that an intensification is coming to an end" (i.e., the peak winds have been reached).

The results of the fixed time lag analysis show that while certain modal times appear to exist, knowledge of which lag to use ahead of time is required to allow prediction. In an effort to provide better predictive power, we have determined the time between the maximum wind and maximum lightning strike rate for each tropical cyclone (using the 6 h resolution time bins). This is subtly different from the cross-correlation analysis which has focused upon matching the intensification and relaxation profile of the wind speeds and lightning strike rates. Table 4 shows the number of tropical cyclones which have their peak winds within a specified time difference from the time of the maximum lightning strike rate. The results show that 31% of the tropical cyclones have their peak winds occurring before the peak in lightning strike rate, such that the lightning peak cannot be used to predict the wind speed peak. Of the 69% of cyclones that have a peak lightning strike rate occurring before the time of the peak winds, almost 25% have a time difference of 24 h or less, while almost a half show a time difference within 48 h. This method of analysis is not as rigorous as the cross-correlation procedure due to reliance on the position of a single data point rather than a profile. However, it does provide a measure of probabilistic prediction.

In this study we have been taking the lightning flash totals at ±3 h either side of the given IBTrACS data time. This does not allow for storm motion in the 3 h giving an error in the distance of each lightning strike from the cyclone center. The cyclone translational speed will vary across individual events and also during the cyclone lifetime. Average tropical cyclone translational speeds range from 4 to 6 m s^{-1} which in a 3 h period corresponds to distances of 43 and 65 km, respectively [e.g., *Kaplan and DeMaria*, 2001; *Elsner et al.*, 2010; *Mei et al.*, 2012]. This error is negligible for the larger radius windows but is obviously important for the smallest 50 km window. It is important to remember though that this error is a maximum and the closer in time to the IBTrACS data point the flash occurs the smaller this positional error will be.

5. Conclusions

We have recreated the Price approach for a set of 58 tropical cyclones but were unable to duplicate the exact results that were found in this study. However, we confirmed their broad conclusions that the observed lightning variability is correlated to wind variability and that on average, the lightning variation leads the wind variation by ~1 day. The Price approach has been extended from the original 3 years of data to an 8 year data set which returns broadly similar lag and correlation results when using a lightning collection window of 10° square or of 500 km radius. The cross-correlation matching between wind and lightning only has an ~8% failure rate. We have calculated both the 10° × 10° square lightning detection window, a radial distance in

kilometers, and performed the lightning to wind cross correlation for a range of circular distances including toroidal rings. The highest correlations were found for the < 300 km radial window with a median linear correlation of 0.8. The calculated lag time for each tropical cyclone using this < 300 km collection window shows a double peak distribution at 0 and +66 h, at this smaller radius a median or mean lag is not appropriate. The eyewall lightning at distances < 50 km from the center of the storm provides only a single peak around a zero time lag.

These results suggest that the predictive timescale of lightning is highly dependent upon which region of the cyclone is investigated. When using a spatially large lightning collection window, our results agree with other studies of high-category tropical cyclones [e.g., *Price et al.*, 2009; *DeMaria et al.*, 2012; *Pan et al.*, 2014] of a ~1 day value. When we look at the region containing the eyewall, we find a 0 day value, indicating that eyewall lightning cannot be used to predict wind intensification using this large temporal-scale binning method. A case by case study looking at much higher time resolutions near the eyewall would be required to look for a potential predictive ability. We note that our results suggest that if such a predictive relationship existed, it would provide no more than 6 h advance warning. When we consider the < 300 km region (rainband and eyewall) we find a double-peaked structure at ~3 days (agreeing with *Pan et al.* [2014] for weak tropical cyclones) and 0 days. This 0 day lag is independent of the eyewall correlation peak, confirmed by the 150–300 km window showing the same double peak structure.

The fixed time lag correlations shown in Table 3 and Figure 7 show that the 66 h time lag provides the highest correlations, and this should be investigated on a set of case studies. The difference in the correlations between the variable and fixed lag, combined with the double modal lag peak, suggests that prior knowledge of which time lag to use is required in order to reliably predict when the peak winds will occur. If the double lightning distribution suggested by *Molinari et al.* [1999] exists, then an estimate of the size of the cyclone will also be an important parameter that is not currently included in the IBTrACS information but could be determined for specific cases where satellite images exist.

References

Abarca, S. F., and K. L. Corbosiero (2011), The World Wide Lightning Location Network and convective activity in tropical cyclones, *Mon. Weather Rev.*, *139*, 175–191, doi:10.1175/2010MWR3383.1.

Black, R. A., and J. Hallett (1986), Observations of the distribution of ice in hurricanes, *J. Atmos. Sci.*, *43*, 802–822, doi:10.1175/1520-0469(1986)043<0802:OOTDOI>2.0.CO;2.

Black, R. A., and J. Hallett (1999), Electrification of the hurricane, *J. Atmos. Sci.*, *56*, 2004–2028, doi:10.1175/1520-0469(1999)056<2004:EOTH>2.0.CO;2.

Brennan, M. J., and S. J. Majumdar (2011), An examination of model track forecast errors for Hurricane Ike (2008) in the Gulf of Mexico, *Weather Forecasting*, *26*, 848–867, doi:10.1175/WAF-D-10-05053.1.

DeMaria, M., J. A. Knaff, and C. Sampson (2007), Evaluation of long-term trends in tropical cyclone intensity forecasts, *Meteorol. Atmos. Phys.*, *97*, 1–4, doi:10.1007/s00703-006-0241-4.

DeMaria, M., J. A. Knaff, and C. Sampson (2012), Tropical cyclone lightning and rapid intensity change, *Mon. Weather Rev.*, *140*, 1828–1842, doi:10.1175/MWR-D-11-00236.1.

Elsner, J. B., R. E. Hodges, and J. C. Malmstadt (2010), *Hurricanes and Climate Change*, Springer, Netherlands.

Emanuel, K. (2005), Genesis and maintenance of "Mediterranean hurricanes", *Adv. Geosci.*, *2*, 217–220, doi:10.5194/adgeo-2-217-2005.

Fierro, A., and J. Reisner (2011), High-resolution simulation of the electrification and lightning of Hurricane Rita during the period of rapid intensification, *J. Atmos. Sci.*, *68*, 477–494, doi:10.1175/2010JAS3659.1.

Hutchins, M. L., R. H. Holzworth, J. B. Brundell, and C. J. Rodger (2012), Relative detection efficiency of the World Wide Lightning Location Network, *Radio Sci.*, *47*, RS6005, doi:10.1029/2012RS005049.

Jacobson, A. R., R. H. Holzworth, J. Harlin, R. Dowden, and E. Lay (2006), Performance assessment of the World Wide Lightning Location Network (WWLLN), using the Los Alamos Sferic Array (LASA) as ground truth, *J. Atmos. Oceanic Technol.*, *23*, 1082–1092, doi:10.1175/JTECH1902.1.

Kaplan, J., and M. DeMaria (2001), On the decay of tropical cyclone winds after landfall in the New England area, *J. Appl. Meteorol.*, *40*, 280–286, doi:10.1175/1520-0450(2001)040<0280:OTDOTC>2.0.CO;2.

Knapp, K. R., M. C. Kruk, D. H. Levinson, H. J. Diamond, and C. J. Neumann (2010), The International Best Track Archive for Climate Stewardship (IBTrACS): Unifying tropical cyclone best track data, *Bull. Am. Meteorol. Soc.*, *91*, 363–376, doi:10.1175/2009BAMS2755.

Lyons, W. A., and C. S. Keen (1994), Observations of lightning in convective supercells within tropical storms and hurricanes, *Mon. Weather Rev.*, *122*, 1897–1916, doi:10.1175/1520-0493(1994)122<1897:OOLICS>2.0.CO;2.

McAdie, C. J., and M. B. Lawrence (2000), Improvements in tropical cyclone track forecasting in the Atlantic basin, *Bull. Am. Meteorol. Soc.*, *81*, 989–998.

Mei, W., C. Pasquero, and F. Primeau (2012), The effect of translation speed upon the intensity of tropical cyclones over the tropical ocean, *Geophys. Res. Lett.*, *39*, L07801, doi:10.1029/2011GL050765.

Molinari, J., P. K. Moore, V. P. Idone, R. W. Henderson, and A. B. Saljoughy (1994), Cloud-to-ground lightning in Hurricane Andrew, *J. Geophys. Res.*, *99*, 16,665–16,676, doi:10.1029/94JD00722.

Molinari, J., P. Moore, and V. Idone (1999), Convective structure of hurricanes revealed by lightning locations, *Mon. Weather Rev.*, *127*, 520–534, doi:10.1175/1520-0493(1999)127.

National Disaster Risk Reduction and Management Council (2014), Updates re effects of TY YOLANDA (HAIYAN). [Available at http://www. ndrrmc.gov.ph/, accessed 27th May 2014, 17 April.]

National Hurricane Center (2014), National Hurricane Center forecast verification. [Available at http://www.nhc.noaa.gov/verification/verify5. shtml, accessed 10th Feb.]

Pan, L., X. Qie, and D. Wang (2014), Lightning activity and its relation to the intensity of typhoons over the Northwest Pacific Ocean, *Adv. Atmos. Sci.*, *31*(3), 581–592, doi:10.1007/s00376-013-3115-y.

Price, C., M. Asfur, and Y. Yair (2009), Maximum hurricane intensity preceded by increase in lightning frequency, *Nat. Geosci.*, *2*, 329–332, doi:10.1038/NGEO477.

Rappaport, E. N., et al. (2009), Advances and challenges at the National Hurricane Center, *Weather Forecasting*, *24*, 395–419, doi:10.1175/2008WAF2222128.1.

Reinhart, B., H. Fuelberg, R. Blakeslee, D. Mach, A. Heymsfield, A. Bansemer, S. L. Durden, S. Tanelli, G. Heymsfield, and B. Lambrigtsen (2014), Understanding the relationships between lightning, cloud microphysics, and airborne radar-derived storm structure during Hurricane Karl, *Mon. Weather Rev.*, *142*, 590–605, doi:10.1175/MWR-D-13-00008.1.

Romps, D. M., J. T. Seeley, D. Vollaro, and J. Molinari (2014), Projected increase in lightning strikes in the United States due to global warming, *Science*, *346*(6211), 851–854, doi:10.1126/science.1259100.

Saffir, H. S. (1973), Hurricane wind and storm surge, *The Military Engineer*, *65*, 423.

Sashoff, S. P., and W. K. Roberts (1942), Directional characteristics of tropical storm static, *Proc. IRE*, *30*, 131–133, doi:10.1109/JRPROC. 1942.234330.

Schiermeier, Q. (2013), Did climate change cause Typhoon Haiyan, *Nature*, doi:10.1038/nature.2013.14139. [Available at http://www.nature. com/news/did-climate-change-cause-typhoon-haiyan-1.14139, accessed 10th Feb 2015.]

Simpson, R. H. (1974), The hurricane disaster potential scale, *Weatherwise*, *27*, 169–186.

Solorzano, N. N., J. N. Thomas, and R. H. Holzworth (2008), Global studies of tropical cyclones using the World Wide Lightning Location Network, *AMS Annual Meeting 2008 in New Orleans,* January 2008.

Thomas, J., N. Solorzano, S. Cummer, and R. Holzworth (2010), Polarity and energetics of inner core lightning in three intense north Atlantic hurricanes, *J. Geophys. Res.*, *115*, A00E15, doi:10.1029/2009JA014777.

Willis, P. T., J. Hallett, R. A. Black, and W. Hendricks (1994), An aircraft study of rapid precipitation development and electrification in a growing convective cloud, *Atmos. Res.*, *33*, 1–24, doi:10.1016/0169-8095(94)90010-8.

Zhang, W., Y. Zhang, D. Zheng, and X. Zhou (2012), Lightning distribution and eyewall outbreaks in tropical cyclones during landfall, *Mon. Weather Rev.*, *140*, 3573–3586, doi:10.1175/MWR-D-11-00347.1.